JGR Atmospheres

RESEARCH ARTICLE
10.1029/2020JD032572

A Laboratory Study on the Isotopic Composition of Hg(0) Emitted From Hg-Enriched Soils in Wanshan Hg Mining Area

Hui Zhang[1,2], Qingyou Tan[1], Leiming Zhang[3], Xuewu Fu[1,4], and Xinbin Feng[1,4]

[1]State Key Laboratory of Environmental Geochemistry, Institute of Geochemistry, Chinese Academy of Sciences, Guiyang, China, [2]University of Chinese Academy of Sciences, Beijing, China, [3]Air Quality Research Division, Science and Technology Branch, Environment and Climate Change Canada, Toronto, Ontario, Canada, [4]CAS Center for Excellence in Quaternary Science and Global Change, Xi'an, China

Abstract Soil Hg(0) emissions are an important source of atmospheric mercury (Hg), but the Hg isotopic signatures of this source remain poorly characterized. In this study, the fractionation of Hg isotopes during Hg (0) emissions from Hg-enriched agricultural and forest soils in Wanshan Hg mining area were investigated through laboratory experiments. Significant mass-dependent fractionation (MDF) of Hg isotopes and mass independent fractionation of odd Hg isotopes (odd-MIF) were observed. Mean MDF enrichment factors ($\varepsilon^{202}Hg_{Hg(0)\text{-}soil}$) of agricultural soil were in the range of −2.03‰ to −1.34‰ for agricultural soil in light-, light moisture-, and temperature-controlled experiments, which were higher than those of forest soil in similar controls (means = −3.38‰ to −1.98‰). Temperature-controlled experiments exhibited a larger MDF compared to light- and light moisture-controlled experiments. Photoreduction of Hg in agricultural soil in the presence and absence of soil water generated a larger positive odd-MIF (mean $E^{199}Hg_{Hg(0)\text{-}soil}$ = 0.67‰ to 0.76‰, n = 2) than the temperature-controlled experiments (mean $E^{199}Hg_{Hg(0)\text{-}soil}$ = 0.18 ± 0.04‰, 1 SD), whereas the $E^{199}Hg_{Hg(0)\text{-}soil}$ of forest soil in temperature controls (mean = 0.23 ± 0.03‰, 1 SD) were higher than that in light (mean = 0.18 ± 0.06‰, 1 SD) and light moisture-controlled experiments (mean = −0.03 ± 0.06‰, 1 SD). It is speculated that photoreducible Hg (II) likely dominantly bound to S-containing ligands in agricultural soil but to both S-containing and sulfurless ligands in forest soil, resulting in significant positive odd-MIF in Hg(0) product during photoreduction in the former case and a small magnitude of positive to some negative odd-MIF in the latter case.

Key Points:
- Soil emitted Hg(0) in all the controlled experiments were characterized by significant negative δ^{202}Hg values (−4.48 to −1.68‰)
- Photoreduction of Hg in agricultural soil had a larger $E^{199}Hg_{Hg(0)\text{-}soil}$ (mean of 0.72‰) than that (mean of 0.18‰) in temperature controls
- Mean $E^{199}Hg_{Hg(0)\text{-}soil}$ of forest soil in temperature control (0.23‰) were higher than that (−0.03~0.18‰) in light and light-moisture controls

Supporting Information:
- Supporting Information S1

Correspondence to:
X. Fu,
fuxuewu@mail.gyig.ac.cn

Citation:
Zhang, H., Tan, Q., Zhang, L., Fu, X., & Feng, X. (2020). A laboratory study on the isotopic composition of Hg(0) emitted from Hg-enriched soils in Wanshan Hg mining area. *Journal of Geophysical Research: Atmospheres*, *125*, e2020JD032572. https://doi.org/10.1029/2020JD032572

Received 10 FEB 2020
Accepted 11 SEP 2020
Accepted article online 15 SEP 2020

Author Contributions:
Conceptualization: Xuewu Fu
Investigation: Hui Zhang, Qingyou Tan, Xuewu Fu
Methodology: Hui Zhang, Qingyou Tan, Xuewu Fu
Writing - original draft: Hui Zhang, Xuewu Fu
Writing – review & editing: Hui Zhang, Leiming Zhang, Xuewu Fu, Xinbin Feng

1. Introduction

Mercury (Hg) is a toxic trace metal pollutant affecting humans and wildlife. Gaseous elemental mercury (Hg(0)) is the dominant form of Hg in the atmosphere (Holmes et al., 2010). Hg(0) has an atmospheric residence time of approximately 0.5–1.0 years and can disperse in the global atmosphere before being deposited to Earth's surfaces or transformed to other atmospheric Hg species (Holmes et al., 2010; Lindberg et al., 2007). Global Hg(0) emissions from primary anthropogenic sources were estimated to be in the range of 1,500 to 1,650 tons annually (AMAP/UNEP, 2013; Streets et al., 2019), and those from natural surfaces were 1.1–4.2 times higher (1,800 to 7,800 tons annually) (Selin, 2009). Naturally Hg-enriched soils, mainly located in the global mercuriferous belts, generally have highly elevated Hg concentrations compared to the background soils (Feng et al., 2013; Gustin et al., 1999). Previous studies reported that emission intensities of Hg(0) were 1–3 orders of magnitude higher from Hg-enriched soils than other natural surfaces (Agnan et al., 2016; Zhu et al., 2016) and total Hg(0) emissions from naturally and anthropogenic contaminated Hg-enriched soils (Hg concentrations > 0.3 μg g^{-1}) accounted for 36% of the global terrestrial Hg(0) emissions (Agnan et al., 2016). Thus, naturally Hg-enriched soils are important sources of Hg(0) and play critical roles in atmospheric Hg budgets, especially at local to regional scales.

Hg has seven stable isotopes in the environment (Hg^{196}, Hg^{198}, Hg^{199}, Hg^{200}, Hg^{201}, Hg^{202}, and Hg^{204}). Significant advances have been made in measuring the Hg isotopic compositions in geological and environmental samples during the past decade (Blum et al., 2014; Sonke & Blum, 2013). Significant mass-dependent fractionation (MDF, δ^{202}Hg signature) and mass-independent fractionation (MIF, Δ^{199}Hg, and Δ^{200}Hg signatures) of Hg isotopes were observed in geological and environmental samples (Blum et al., 2014). MDF of

Hg isotopes could be caused by many natural processes including aqueous reduction and oxidation, gaseous-phase oxidation, soil adsorption, photoreduction of particulate bound mercury, and foliar/air exchange of Hg (Demers et al., 2013; Fu et al., 2019; Jiskra et al., 2012; Sun et al., 2016; Wiederhold et al., 2010; Zheng et al., 2018), whereas MIF of Hg isotopes is mainly induced by photochemical reactions (Bergquist & Blum, 2007; Chen et al., 2012; Fu et al., 2019; Gratz et al., 2010; Motta et al., 2020; Zheng & Hintelmann, 2009). MIF of Hg isotopes is considered as related to the magnetic isotope effect (MIE) and the nuclear volume effect (NVE) (Buchachenko et al., 2004; Schauble, 2007). Despite our incomplete understanding of the mechanisms associated with MDF and MIF of Hg isotopes in various geological and environmental processes, isotope fractionation of Hg, especially MIF, is a powerful tool in tracking Hg transformation and reaction mechanisms.

Exchange of Hg between soil and atmosphere plays an important role in the biogeochemical cycling of Hg; however, fractionation of Hg isotopes during this process has not been well characterized. Processes involved in the fractionation of Hg isotopes associated with soil-atmosphere exchange of Hg likely include photochemical/biotic/abiotic reduction and oxidation, adsorption, and desorption (Zhang & Lindberg, 1999). Demers et al. (2013) observed that Hg(0) emitted from forest soil to the atmospheric pool had very positive δ^{202}Hg (0.60‰ to 1.60‰) and moderate negative Δ^{199}Hg (−0.25‰ to −0.12‰), which were likely related to the adsorption and/or oxidation of Hg(0) in the surface soil ecosystem. However, studies on the isotopic composition of Hg in forest soil depth profiles observed a consistent increase of δ^{202}Hg value with increasing soil depth that was partly attributed to the preferential loss of lighter Hg isotopes during abiotic dark reduction (Jiskra et al., 2015; Zheng et al., 2016). In addition, recent studies reported an enrichment of lighter Hg isotopes in reactant Hg(0) in soil pore air and natural water during abiotic dark oxidation (negative MDF of Hg isotopes) (Jiskra et al., 2019; Zheng et al., 2018). These latter studies indicated that nonphotochemical abiotic reduction and oxidation tend to enrich in lighter Hg isotopes in soil air Hg(0) pool. It should be noted that the biological/physicochemical nature and Hg contents of soils vary significantly at local, regional, and global scales, which would affect the biogeochemical cycling of Hg at the soil-atmosphere interface and would likely further induce different fractionation patterns during soil-atmosphere exchange of Hg. Therefore, there is a need to more widely study the Hg isotope fractionation between soil and atmosphere in different environmental settings in order to better understand the biogeochemical cycling of Hg within various soil ecosystems and evaluate the effects of soil emissions on the isotopic signatures of atmospheric Hg(0) pool.

The Wanshan Hg mining area in Guizhou province of Southwest China had a long history of Hg mining until the complete prohibition of large-scale Hg mining in 2004. Historical Hg mining has already resulted in severe Hg pollution in this region (Wang et al., 2007). Soil Hg concentrations in this area are highly elevated (up to 2–4 orders of magnitude) compared to national background levels. Emission fluxes of Hg(0) in Wanshan Hg mining area (means: 160–27,800 ng m^{-2} hr^{-1}) were also much higher than those observed in background areas, enabling this area to be a strong source of atmospheric Hg(0) at local and regional scales (Wang et al., 2007). In this study, the isotopic compositions of Hg(0) emitted from agricultural rice paddy soil (Hg concentration = 218 ± 19.2 μg g^{-1}, 1 SD) and forest soil (Hg concentration = 15.4 ± 0.4 μg g^{-1}, 1 SD) collected from the Wanshan Hg mining area were measured in the laboratory. The objectives of this study were to (1) characterize the isotopic compositions of Hg(0) emitted from Hg-enriched soils in Hg mining area and (2) evaluate the factors influencing the fractionation of Hg isotopes during Hg(0) emission from soil.

2. Materials and Methods

2.1. Soil Sample Collection and Processing

Soil samples were collected from surface soil layer (0–5 cm) at two different sites: a rice paddy field (also referred to as agricultural soil below) and a forest field in the Wanshan Hg mining area, Guizhou, southwest China. The rice paddy field was located in a river valley and frequently impacted by contaminated river water and runoff that leached Hg from mine-waste calcines and/or unroasted cinnabar ore waste (Qiu et al., 2005). The forest field was located in a mountainous slope where there was no impact of mining waste, and the sources of Hg should be mainly related to atmospheric deposition and parent rock. All samples were immediately sealed with three successive polyethylene bags. In the laboratory, soil samples were freeze-dried, milled (~100 mesh), and sealed in two successive polyethylene bags and kept in a refrigerator at 2–4°C

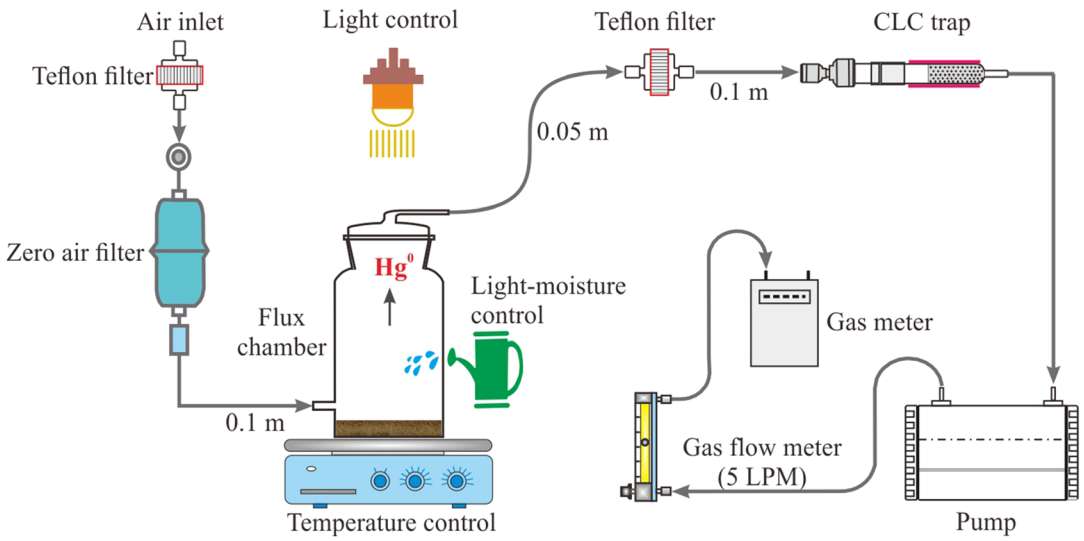

Figure 1. Collection of Hg(0) emitted from soil for Hg isotope analysis.

until flux measurements and isotope analysis. Microscopic analysis with the Transmission Electron Microscope (TEM, FEI Inc.) and Energy Dispersive X-Ray Spectroscopy (EDX, EDAX Inc.) indicates that Hg compounds in the agricultural soil may partly include Nano HgS, microscopic balls of liquid or colloidal Hg(0), and Hg-Al-Au-Ni amalgams or HgO adsorbed on clay minerals (Figure S1 in the supporting information). A previous study suggested that the microscopic balls of liquid and colloidal Hg(0) and gaseous Hg(0) in sediments impacted by mine waste drainages represent a small fraction of the total Hg (<0.1%) (Bloom et al., 2003; Dreyfr, 1939; Gray et al., 2000; Jew et al., 2011). The native gaseous Hg(0) is soil samples might be lost during soil processing, but the bulk of the microscopic balls of liquid and colloidal Hg(0), which were coated with gas-impervious layer (Bloom et al., 2003), should be preserved.

2.2. Hg(0) Flux Emitted From Soils

Hg(0) emitted from soils was collected at the outlet of a dynamic flux chamber (DFC) using a 600 mg chlorine-impregnated activated carbon (CLC) trap at a flow rate of 5 L min^{-1} (Figure 1) (Fu et al., 2014). A Teflon filter (pore size 0.2 μm) and a Tekran zero air filter were connected in sequence to the DFC to remove air particles and Hg from inlet air, allowing us to collect Hg(0) emitted from soil and isolate the deposition of Hg(0) to soil. Therefore, the measurements conducted in this study are primarily representative of the Hg isotope fractionation during soil Hg(0) emissions rather than the bidirectional exchange between soil and atmosphere. The chamber is made of quartz glass with a thickness of 1 mm and a size of 10 cm in diameter and 15 cm in height. For each agricultural soil experiment, 10 g agricultural soil was added into the chamber, while 2.5 g forest soil was used for each forest soil experiment because forest soil had a much lower density than agricultural soil. The amount of soils used in this study enabled sufficient collection of Hg(0) for Hg isotope analysis and avoided resuspension of soil particle within the chamber. The use of different amount of soils yielded uncertainties in intercomparison of emission flux of Hg(0) between the forest soil and agricultural soil but would not affect the intercomparison of Hg(0) isotope compositions because they were independent on the fractions of Hg lost from soil when they were lower than <1.1% (Tables S1 and S2). During the experiment, Hg(0) emitted from soil was carried off by the Hg-free air and subsequently collected by the CLC trap at a flow rate of 5 L min^{-1} (5 LPM). No visible resuspension of soil particle within the chamber and condensation of soil water on the wall of the chamber were observed during the experiment. A Teflon filter (pore size of 0.2 μm) was utilized immediately at the outlet of the chamber, which was used, just in case, to remove air particles that might be generated during the experiment. During the sampling period, the CLC trap was kept warm (~70°C) using silicone rubber heating pads to prevent water condensation. Hg(0) concentrations at the chamber outlet were continuously measured using an automated Tekran 2537B Hg vapor analyzer at 5 min interval, which was used to collected known amounts of Hg(0) emitted from soils (Tables S1 and S2). After the completion of collection, the CLC trap was sealed with silicone

stoppers and three successive polyethylene bags and stored in a clean lab for 1–3 weeks until preconcentration into trap solutions for Hg isotope analysis.

Blank values of CLC determined by a DMA-80 automatic mercury analyzer were 0.27 ± 0.06 ng g^{-1} (mean ± 1 SD, $n = 8$). A CLC trap that contains 600 mg of CLC therefore had a mean Hg blank of 0.16 ng, which is negligible (<1.2%) compared to the typical quantity (>15 ng) of Hg collected in the trap. Breakthrough of the CLC traps were investigated in the laboratory at the flow rate of 5 L min^{-1} over 24 hr following the method by Fu et al. (2014), which ranged from 0.07% to 0.83% (mean = 0.35 ± 0.29%, 1 SD, $n = 6$). The recoveries of the collected Hg(0) using the experimental setting were investigated by injections of known amounts of Hg(0) vapor (8.6–49.0 ng) at the inlet of the chamber at room temperature. The recoveries ranged from 88% to 112% (mean = 93.4 ± 7.7%, 1 SD, $n = 8$), which would not likely result in significant bias in measurements of Hg(0) isotopic compositions (Fu et al., 2014).

In the laboratory, the isotopic composition of Hg(0) emitted from soil was investigated under three categories of controlled experiments: (1) light control-light exposure at room temperature and zero soil moisture; (2) temperature control-soil temperature at approximately 40°C, 100°C, and 130°C in the absence of light and soil moisture; and (3) light moisture control-soil moisture at 5%, 10%, 20%, and 30% in the presence of light and at room temperature. Note that temperature control experiment at room temperature (e.g., ≤30°C) was not conducted because soil emitted Hg(0) under this condition in 1-week time was not sufficient for Hg isotope analysis. Light exposure control was accomplished by using a Mercury Light Source (Newport, USA) equipped with a 350 W mercury arc lamp and fused silica lenses. The Mercury Light Source generated mainly UVA and UVB light and visible light (290 to 850 nm with the peak of 366 nm; Figure S2). The quartz glass flux chamber allowed to transmit 85% UVA and UVB and 89% visible light (Figure S2). Soil temperature was controlled by a Teflon coated digital hotplate. The surface temperatures of the hotplate were routinely measured using a calibrated digital thermometers and were close to the settings (within ±4°C). Soil moisture control was accomplished by adding Mill-Q water (18.2 MΩ cm) into soil at designated mass ratio (g/g) of water to soil at the beginning of each experiment. We caution that, due to facts that soils was processed (e.g., freeze-dried and milled), soil moisture contents might be decreased from the initially designated settings during light moisture control experiment, and temperatures utilized during temperature control (e.g., 100°C and 130°C) were much higher than the soil temperatures under natural conditions, the isotopic composition of Hg(0) emitted from soils in this study should be more likely regarded as a qualitative indication.

2.3. Sample Processing for Hg Concentration and Isotope Analysis

Before Hg concentration and isotope analysis, Hg(0) collected on CLC traps and Hg in soils were preconcentrated into 5–10 ml of 40% mix acid solution (v/v, $2HNO_3$/1HCl) using a double-stage combustion protocol described in literature (Fu et al., 2014; Sun et al., 2013). Briefly, CLC and soil were combusted in a Hg-free oxygen flow (25 ml min^{-1}), and then the combustion products were further decomposed in a hot quartz tube (1,000°C). Hg(0) collected on CLC traps and Hg in soils were released in the form of Hg(0), which was subsequently trapped by the mixed acid solution. After combustion, Milli-Q water was used to rinse the trapping bottles and impingers three times and added the rinse water to the final trapping solutions to yield an acid concentration of ~20%. The final trapping solution was kept in a refrigerator at 2–4°C until the Hg concentration and isotope analysis. Blanks of the combustion system were determined by combustion of 600 mg of CLC and showed a mean value of 0.03 ± 0.004 ng ml^{-1} ($n = 3$), which was negligible compared to the trap solutions (>1 ng ml^{-1}). Combustion of certified reference materials BCR 482 (Lichen, 480 ng g^{-1}) and NIST-2711 (Montana soil, 7 ug g^{-1}) showed mean recoveries of 95.7 ± 3.2% and (1 SD, $n = 6$) and 98.7 ± 4.6% (1 SD, $n = 10$), respectively.

2.4. Hg Concentrations, Total Organic Matter, and Total Sulfur in Soil and Soil Hg(0) Emission Flux

Soil Hg concentration was determined using a DMA-80 automatic mercury analyzer. Duplicate measurements were conducted in each case and mean values are shown in this study. Hg concentration in trapping solution was determined using a cold vapor atomic fluorescence spectrometry (CVAFS, Model 2500, Tekran Instruments, Canada) following the US-EPA Method 1631 (USEPA, 2002). Hg(0) concentration in outflow of the DFC was calculated by dividing the total mass of Hg(0) collected by the total sampling air volume

measured by gas meter (Figure 1). The measured total sampling volumes showed negligible bias (<5%) with that calculated from the designated flow rate setting (5 L min^{-1}) and sampling duration. Contents of natural organic matter (NOM) in the soils were analyzed using KCr_2O_7 (potassium dichromate) oxidation coupled with volumetric analysis (Meng et al., 2016). Contents of total sulfur (S) in the soils were determined using ICP-AES following *aqua regia* digestion (Salminen et al., 2005).

Hg(0) emission flux from soil was calculated using Equation 1:

$$F = C_o \times Q \div A, \tag{1}$$

where F is the Hg(0) flux in ng m^{-2} hr^{-1}; C_0 is the Hg(0) concentration of DFC outlet air in ng m^{-3}; Q is the flow rate through the DFC in m^3 hr^{-1}; and A is the surface area of soil in DFC in m^2.

2.5. Mercury Isotope Analysis

Hg isotope ratios were measured using cold vapor multicollector inductively coupled plasma mass spectrometry (CV-MC-ICPMS, Nu Plasma, Nu Instruments, UK) following the method described in previous studies (Yin et al., 2010). Before Hg isotope analysis, each trapping solution sample was diluted to Hg concentration of ~1 ng ml^{-1}. Diluted trapping solution and $SnCl_2$ (3%) were mixed online and introduced into a custom-made continuous flow cold-vapor generation and liquid-gas separation system (Lin et al., 2015), and then the isotope ratios of the reduced Hg(0) were measured by the MC-ICPMS. Instrumental mass bias was corrected by standard-sample-standard bracketing using NIST SRM 3133 Hg (NIST, USA) at matching concentrations (<10%) and an internal Tl standard (NIST 997, NIST, USA). Diluted NIST SRM 3133 and 3177 (Mercuric Chloride Standard Solution) standard solutions were prepared using 20% mix acid solution (v/v, $2HNO_3$/1HCl). Delta notation (δ) was used to report MDF values, which is the per mil deviations in Hg isotope ratios of sample relative to the NIST 3133 Hg standard (Blum & Bergquist, 2007):

$$\delta^{xxx}Hg(‰) = \left[\frac{\left(\frac{^{xxx}Hg}{^{198}Hg}\right)_{sample}}{\left(\frac{^{xxx}Hg}{^{198}Hg}\right)_{NIST\ SRM\ 3133}} - 1\right] \times 1,000, \tag{2}$$

where *xxx* refers to the mass of each Hg isotope between 199 and 202 (Hg^{204} was not measured because of the limitations of instrumental collector designs). MIF values are expressed by "capital delta (Δ)" notation (‰) (Bergquist & Blum, 2007):

$$\Delta^{199}\mathrm{Hg}\ (‰) = \delta^{199}\mathrm{Hg} - \left(0.252 \times \delta^{202}\mathrm{Hg}\right), \tag{3}$$

$$\Delta^{200}\mathrm{Hg}\ (‰) = \delta^{200}\mathrm{Hg} - \left(0.502 \times \delta^{202}\mathrm{Hg}\right), \tag{4}$$

$$\Delta^{201}\mathrm{Hg}\ (‰) = \delta^{201}\mathrm{Hg} - \left(0.752 \times \delta^{202}\mathrm{Hg}\right). \tag{5}$$

A standard reference NIST SRM 3177 was analyzed repeatedly to obtain the analytical uncertainty of isotopic compositions during instrumental procedures. The mean values of δ^{202}Hg, Δ^{199}Hg, Δ^{200}Hg, and Δ^{201}Hg for all NIST SRM 3177 standard were −0.51 ± 0.13‰, −0.01 ± 0.06‰, 0.01 ± 0.05‰, and −0.01 ± 0.08‰ (2 SD, n = 30), respectively, which are in agreement with previously reported values (Fu, Zhang, Feng, et al., 2019; Sun et al., 2016). In addition, isotopic compositions of standard references of BCR 482 (δ^{202}Hg = −1.63 ± 0.19‰; Δ^{199}Hg = −0.58 ± 0.08‰; Δ^{200}Hg = 0.07 ± 0.08‰; and Δ^{201}Hg = −0.60 ± 0.12‰, 2 SD; n = 6) and NIST 2711 (δ^{202}Hg = −0.18 ± 0.08‰; Δ^{199}Hg = −0.24 ± 0.05‰; Δ^{200}Hg = 0.00 ± 0.05‰; and Δ^{201}Hg = −0.18 ± 0.08‰, 2 SD, n = 10) were also measured and agreed with previously published results (Biswas et al., 2008; Blum & Johnson, 2017; Estrade et al., 2010; Smith et al., 2015; Wiederhold et al., 2013). Such an agreement together with the nearly complete recovery of Hg in standard references mentioned above indicate the preconcentration method used in this study would not induce significant bias in measurements of Hg isotope compositions. The analytical uncertainty (2 SD) of Hg isotopic compositions in the study is the larger 2 SD value of either the repeated analysis of the sample or the procedural NIST 3177.

3. Results and Discussion

3.1. Soil Hg Concentration and Emission Flux

Concentrations of Hg in the agricultural and forest soils were 218 ± 19.2 μg g^{-1} and 15.4 ± 0.4 μg g^{-1} (1 SD), respectively, which are significantly higher than those of the background soils (e.g., <0.3 μg g^{-1}) (Agnan et al., 2016). NOM contents were 4.2% and 6.9% of soil mass, and Hg/NOM ratios were 5.2 × 10^5 ng/mg and 2.2 × 10^3 ng/mg for the agricultural soil and forest soil, respectively. Average total sulfur contents of the agricultural soil and forest soil were 341 ± 14 mg kg^{-1} and 472 ± 11 mg kg^{-1} (1 SD), respectively.

Soil Hg(0) emission fluxes varied significantly under different laboratory-controlled conditions (Tables S1 and S2). Hg(0) emission fluxes from the agricultural soil increased by more than 2 orders of magnitude (from 23.5 to 5,648 ± 2,606 or 14,675 ± 4,202 ng m^{-2} hr^{-1}, 1 SD) when soil temperature increased from 40°C to 100°C or 130°C. The phenomenon of increasing Hg(0) emission flux with increasing temperature has also been reported in previous studies (Choi & Holsen, 2009; Gustin et al., 1997), which is likely due to the increasing vapor pressure of volatile Hg(0) and a decreasing sorption by soil, but also an acceleration of abiotic reduction processes at higher temperatures (Gustin et al., 2004; Schluter, 2000). No significant difference in Hg(0) emission flux from the agricultural soil was observed between the light moisture (10%) control experiments (mean = 580 ± 160 ng m^{-2} hr^{-1}) and light control experiments (mean = 804 ± 533 ng m^{-2} hr^{-1}) when the fractions of released Hg(0) ranged from 0.09‰ to 0.46‰ (two-independent sample *t* test, $p = 0.92$; Table S1). On the other hand, Hg(0) emission fluxes from the agricultural soil in the light moisture (5% to 30%) control experiments (1,413 to 2,405 ng m^{-2} hr^{-1}) were 1.7 to 2.9 times higher than in the light control experiments (829 ng m^{-2} hr^{-1}) when a smaller fraction of Hg was released from soil (i.e., 0.007‰; Table S1). These results suggest that soil Hg(0) emission could be enhanced immediately after water addition (e.g., <1.4 hr), but such an enhancement would be significantly suppressed with increasing sampling durations (e.g., >15 hr) due to decreasing soil moisture content with time (Gustin & Stamenkovic, 2005; Lindberg et al., 1999). Soil Hg(0) emissions in the light control experiments were mainly controlled by photochemical reduction, as can be seen from the much higher fluxes (35 to 102 times; Table S1) from the experiments with light (light control and light moisture control at room temperature) than without light (temperature control at 40°C), which is consistent with previous studies (Fantozzi et al., 2013; Moore & Carpi, 2005).

Soil moisture seemed to play little role in modulating Hg(0) emission from the forest soil, as can be seen from the insignificant difference in emission flux between the light control (41.0 ± 14.5 ng m^{-2} hr^{-1}, 1 SD) and light moisture (10%) control (40.9 ± 14.3 ng m^{-2} hr^{-1}, 1 SD) experiments (two-independent sample *t* test, $p = 1.00$; Table S2). High soil temperature substantially enhanced Hg(0) emission from the forest soil, for example, Hg(0) emission flux of 25,928 ± 11,470 ng m^{-2} hr^{-1} (1 SD) at 130°C, which was approximately 3 orders of magnitude higher than those in the light control and light moisture control experiments (Table S2). Hg(0) emission flux from the forest soil was under the detection limit in the absence of light and at room temperature, indicating photochemical reduction controlled emissions of Hg(0) in the light control and light moisture control experiments.

A significant variation in Hg(0) emission fluxes from agricultural and forest soils was observed for each category of controlled experiments (chi-square test, *p* values for all <0.01; Tables S1 and S2). As shown in Tables S1 and S2, Hg(0) emission fluxes from agricultural soil in light- and light moisture-controlled experiments and from forest soil in light-, light moisture-, and temperature-controlled experiments decreased with the fraction of Hg(0) emitted from soils. It is speculated that some reducible Hg species in agricultural and forest soils were preferentially lost at the beginning of the progressing experiments, causing initially rapid emissions observed in our experiments. These reducible Hg species should be coordinated with both sulfurless and S-containing ligands (characterized by negative and positive MIF in Hg(0) product, respectively; Zheng & Hintelmann, 2010a), as evidenced by the small variations in MIF signatures of emitted Hg(0) during each progressing experiment, with the exception of agricultural soil in light moisture-controlled experiments (characterized by initially higher positive MIF in Hg(0) product). The small variations in MIF signatures of emitted Hg(0) also indicates a small effect of evaporation of elemental Hg on the variations of Hg(0) emission flux from the agricultural soil in light- and light moisture-controlled experiment, which generally generates much smaller magnitude of positive MIF in Hg(0) product than photochemical processes (Estrade et al., 2009). However, the effect of elemental Hg evaporation could not be excluded for the temperature-controlled experiments, since the magnitude of MIF caused by

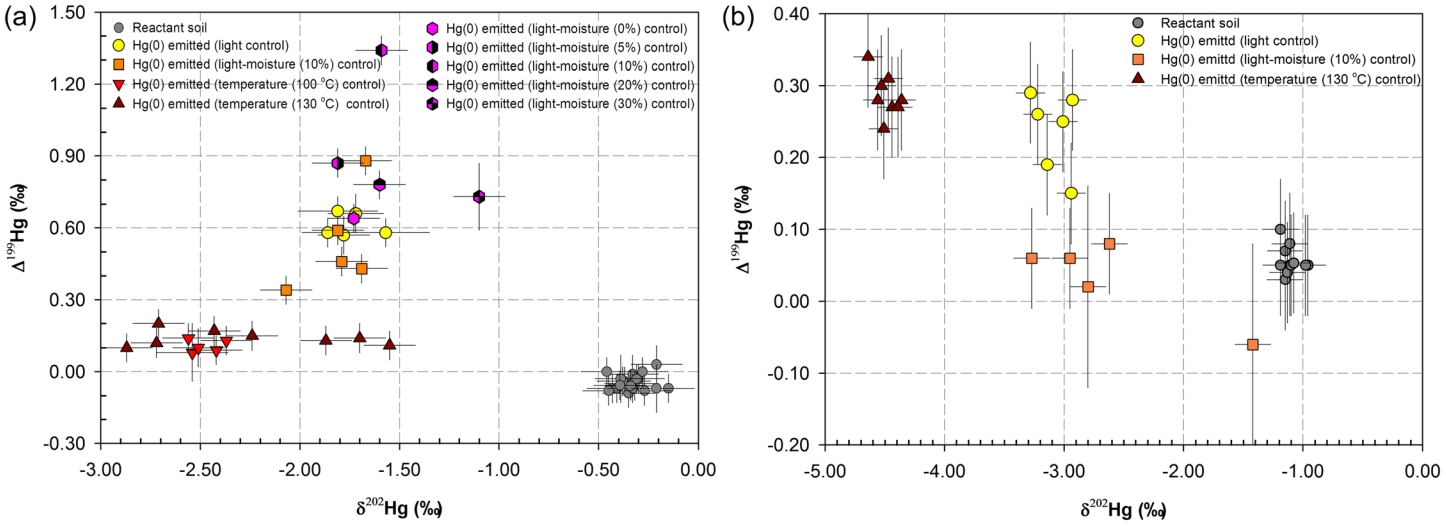

Figure 2. δ^{202}Hg and Δ^{199}Hg values of emitted Hg(0) and reactant soils for agricultural soil (a) and forest soil (b) in this study. Error bars are 2σ analytical uncertainty isotopic composition.

liquid-vapor Hg(0) evaporation is more or less similar to that caused by nonphotochemical processes (Estrade et al., 2009; Zheng & Hintelmann, 2010b).

3.2. Isotopic Compositions of Reactant Soil

During all progressing experiments, Hg lost from reactant agricultural and forest soils account for a small fraction of Hg in the initial soils (<1.1%; Tables S1 and S2). The isotopic compositions of reactant agricultural (δ^{202}Hg = −0.56‰ to −0.15‰, Δ^{199}Hg = −0.09‰ to 0.02‰, n = 23) and forest soils (δ^{202}Hg = −1.19‰ to −0.96‰, Δ^{199}Hg = 0.03 to 0.10, n = 10), were statistically consistent with that of the initial soils (one-sample t test, p = 0.10 to 0.31; Figure 2 and Tables S1 and S2). The mean (±1 SD) δ^{202}Hg and Δ^{199}Hg values of the initial and reactant agricultural soil were −0.34 ± 0.08‰ and −0.05 ± 0.03‰ (n = 24). A previous study by Feng et al. (2013) proposed that Hg in agricultural soils in Wanshan Hg mining area were likely derived from a mixing of Hg ores and Hg waste calcines, based on their analogous Hg MDF signatures. However, Δ^{199}Hg of agricultural soil in the present study was slightly but significantly lower than that of Hg cinnabar ores and Hg waste calcines (mean Δ^{199}Hg = 0.01 ± 0.02‰, 1 SD, n = 24) (two-independent sample t test, $p < 0.01$; Yin et al., 2013), which could be partially caused by photoreduction of S-bound Hg (II) in agricultural soils that depletes odd Hg isotopes (more details below).

The forest soil investigated here had mean (±1 SD) δ^{202}Hg and Δ^{199}Hg values of −1.10 ± 0.08‰ and 0.06 ± 0.02‰ (n = 11), respectively. δ^{202}Hg and Δ^{199}Hg values of the forest soil were approximately 0.30‰ to 0.95‰ and 0.23‰ to 0.41‰ higher than those of the global background forest surface soils (mean δ^{202}Hg = −2.05‰ to −1.40‰, mean Δ^{199}Hg = −0.36‰ to −0.18‰) (Demers et al., 2013; Jiskra et al., 2015; Wang et al., 2017; Zheng et al., 2016), respectively. Given that Hg in forest soils are mainly derived from deposition of litter that uptakes Hg(0) from the atmosphere (66% to 90%) (Enrico et al., 2016; Jiskra et al., 2015; Zheng et al., 2016), the above results may indicate a positive Δ^{199}Hg signature of atmospheric Hg(0) in the study area, which agrees with the positive Δ^{199}Hg signatures of Hg(0) emitted from the agricultural and forest soils observed in this study (more details below). However, contributions of parent rock and atmospheric Hg (II) deposition (characterized by significant positive Δ^{199}Hg (Fu, Zhang, Feng, et al., 2019; Sun et al., 2019) to forest soil in the study area cannot be ruled out.

3.3. MDF of Hg(0) Isotope

Soil emitted Hg(0) in both the agricultural and forest soil experiments were characterized by significant negative δ^{202}Hg values, although with higher values from agricultural soil (means = −2.37‰ to −1.68‰, n = 3) than forest soil (means = −4.49‰ to −2.61‰, n = 3) in light-, light moisture-, and temperature-controlled experiments (Figure 2 and Tables S1 and S2). This could be partially attributed to the less negative

Table 1
Summary of Soil Hg(0) Emission Flux, Fraction of Hg Emitted From Reactant Soil, and Hg Isotope Enrichment Factors for MDF (i.e., $\varepsilon^{202}Hg_{Hg(0)\text{-}soil}$) and MIF ($E^{199}Hg_{Hg(0)\text{-}soil}$, $E^{200}Hg_{Hg(0)\text{-}soil}$, and $E^{201}Hg_{Hg(0)\text{-}soil}$) During Hg(0) Emissions From Agricultural and Forest Soils in the Light-, Light Moisture-, and Temperature-Controlled Experiments

Soil type	Environmental condition	n	Fraction of Hg emitted (%)	Hg(0) flux (ng m^{-2} hr^{-1})			$\varepsilon^{202}Hg_{Hg(0)\text{-}soil}$ (‰)			$E^{199}Hg_{Hg(0)\text{-}soil}$ (‰)			$E^{200}Hg_{Hg(0)\text{-}soil}$ (‰)			$E^{201}Hg_{Hg(0)\text{-}soil}$ (‰)		
				Range	Mean	1 SD	Range	Mean	1 SD	Range	Mean	1 SD	Range	Mean	1 SD	Range	Mean	1 SD
Agricultural soil	Light control	6	0.0007 to 0.046	499 to 1,739	808	477	−1.52 to −1.23	−1.40	0.10	0.62 to 0.72	0.67	0.05	−0.02 to 0.03	0.02	0.02	0.61 to 0.74	0.67	0.06
	Light moisture (5%, 10%, 20%, and 30%) control	9	0.0007 to 0.046	341 to 2,405	1,139	719	−1.73 to −0.76	−1.34	0.26	0.39 to 1.39	0.76	0.31	−0.03 to 0.03	0.01	0.02	0.38 to 1.30	0.75	0.29
	Temperature (40°C, 100°C, and 130°C) control	16	0.0007 to 0.184	23.5 to 20,216	9,841	6,088	−2.53 to −1.21	−2.03	0.38	0.13 to 0.26	0.18	0.04	−0.01 to 0.09	0.02	0.02	0.02 to 0.25	0.11	0.05
Forest soil	Light control	6	0.065 to 0.390	23.3 to 67.0	41.0	14.5	−2.17 to −1.82	−1.98	0.15	0.09 to 0.23	0.18	0.06	−0.02 to 0.09	0.02	0.04	0.15 to 0.25	0.21	0.04
	Light moisture (10%) control	5	0.065 to 0.325	26.5 to 62.6	40.9	14.3	−2.16 to −0.31	−1.51	0.71	−0.12 to 0.02	−0.03	0.06	−0.02 to 0.07	0.02	0.04	−0.03 to 0.15	0.10	0.07
	Temperature (130°C) control	8	0.130 to 1.04	12,784 to 41,610	25,928	11,470	−3.53 to −3.25	−3.38	0.09	0.18 to 0.28	0.23	0.03	0 to 0.06	0.03	0.02	0.10 to 0.19	0.14	0.04

Note. MDF and MIF enrichment factors are defined as the difference between the isotopic composition of Hg(0) production and the isotopic composition of Hg in reactant soil. The MDF and MIF signatures of Hg in reactant soils during our progressing experiments are identical to that in initial soils because of the small fraction (<1.1%) of Hg lost from soils. Therefore, Hg isotope enrichment factors for MDF and MIF could not be calculated using the Rayleigh model.

δ^{202}Hg signatures of agricultural soil. However, the average MDF enrichment factors ($\varepsilon^{202}Hg_{Hg(0)\text{-}soil} = \delta^{202}Hg_{Hg(0)} - \delta^{202}Hg_{soil}$) of agricultural soil (−2.03‰ to −1.34‰, $n = 3$) in light-, light moisture-, and temperature-controlled experiments were higher than those of the forest soil (−3.38‰ to −1.51‰, $n = 3$) (Table 1), indicating that the magnitude of Hg MDF during its emissions from soils was likely affected by soil matrix, with a higher magnitude of negative MDF associated with emissions of Hg(0) from the forest soil as compared to the agricultural soil.

The direction of MDF in this study is overall similar to those found in previous studies on evaporation of Hg(0) from liquid mercury and solutions as well as photochemical and nonphotochemical reduction of Hg in solutions, foliage, and building surface (Bergquist & Blum, 2007; Estrade et al., 2009; Ghosh et al., 2013; Jiskra et al., 2019; Yuan et al., 2019; Zheng et al., 2007; Zheng & Hintelmann, 2009, 2010a, 2010b). This is overall consistent with the kinetically process-induced isotope fractionation that enriches the lighter isotopes in Hg(0) product. Mean $\varepsilon^{202}Hg_{Hg(0)\text{-}soil}$ values of agricultural (−1.40‰ and −1.34‰) and forest soils (−1.98‰ and −1.51‰) in light and light moisture experiments were similar to those of photochemical reductions of Hg (II) in solution (−2.00‰ to −0.40‰) (Bergquist & Blum, 2007; Kritee et al., 2008; Yang & Sturgeon, 2009; Zheng & Hintelmann, 2009), but lower than those of Hg(0) evaporation from solution (−0.74‰ to −0.65‰) and from liquid mercury under equilibrium conditions (−1.21‰ to −0.86‰) (Estrade et al., 2009; Ghosh et al., 2013; Zheng et al., 2007) and much higher than those of dynamic evaporation of Hg(0) from liquid mercury (mean = −6.7‰) (Estrade et al., 2009). As discussed earlier, Hg(0) emission driven by nonphotochemical reduction and evaporation processes at room temperature (e.g., ≤40°C) contributed insignificantly (e.g., <3%) to the total emission flux in light- and light moisture-controlled experiments, it is therefore proposed that the MDF of Hg(0) isotopes was mainly affected by photochemical reduction of Hg (II). The linear correlations between Δ^{199}Hg and δ^{202}Hg values in Hg(0) product and reactant soils in light- and light moisture-controlled experiments yielded $\Delta^{199}Hg/\delta^{202}Hg$ ratios of −0.48 to −0.35 and −0.09 to −0.01 for agricultural and forest soils, respectively. These values were higher than that observed in photoreduction of Hg (II) bound to S-containing ligands (−0.77; Zheng & Hintelmann, 2010a) and lower than in photoreduction of Hg (II) bound to sulfurless ligands (1.2; Bergquist & Blum, 2007), indicative of a combined result of photoreception of Hg (II) bound to various NOM (e.g., S-containing and sulfurless ligands).

Temperature-controlled experiments displayed a larger negative Hg MDF than light- and light moisture-controlled experiments. For example, mean $\varepsilon^{202}Hg_{Hg(0)\text{-}soil}$ of agricultural soil in temperature-controlled experiments was −2.03 ± 0.38‰ (1 SD, $n = 16$), which is 0.63‰ and 0.69‰ lower than the means in light or light moisture-controlled experiments, respectively (Table 1). For the forest soil, the mean $\varepsilon^{202}Hg_{Hg(0)\text{-}soil}$ in temperature-controlled experiments was −3.38 ± 0.09‰ (1 SD, $n = 8$), which is 1.40‰ and 1.87‰ lower than the means in light or light moisture-controlled experiments, respectively (Table 1). $\Delta^{199}Hg/\delta^{202}Hg$ ratios in temperature-controlled experiments were −0.08 ± 0.01 and −0.07 ± 0.01 (1 SD) for the agricultural and forest soils, respectively, similar to those determined from abiotic dark reductions of Hg (II) (−0.13 to 0) (Bergquist & Blum, 2007; Zheng & Hintelmann, 2010b), equilibrium (−0.14 to −0.12) and dynamic (−0.01) evaporation of Hg(0) from liquid mercury (Estrade et al., 2009; Ghosh et al., 2013). Since nonphotochemical reductions of Hg (II) generally generate similar magnitude of Hg MDF as photochemical reductions of Hg (II) (Sun et al., 2019, and references therein), it is speculated that the larger magnitude of negative MDF in temperature-controlled experiments might be attributed to dynamic emission of liquid and colloidal elemental Hg in soils (characterized by large magnitude of negative

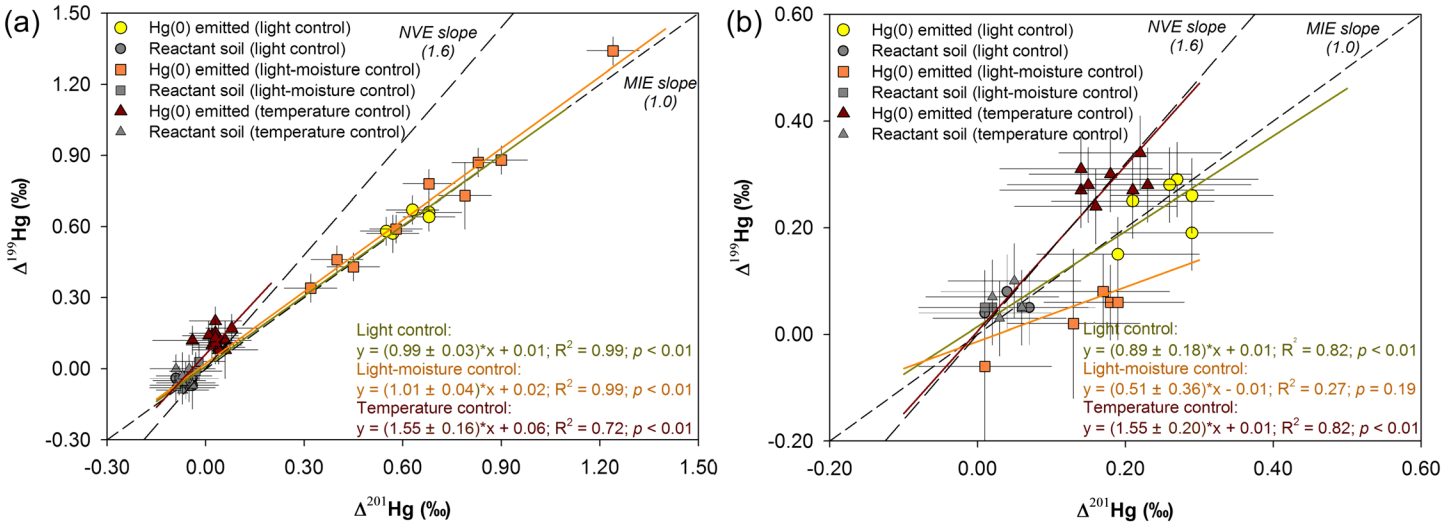

Figure 3. Δ^{199}Hg versus Δ^{201}Hg during emission of Hg(0) from agricultural (a) and forest soils (b) in light-, light moisture-, and temperature-controlled experiments. Error bars are 2 SD analytical uncertainty of Δ^{199}Hg and Δ^{201}Hg. The linear regression between Δ^{199}Hg and Δ^{201}Hg was calculated using Williamson-York iterative bivariate regression with analytical uncertainty (York et al., 2004). MIE and NVE slopes are adopted from literature (Bergquist & Blum, 2007; Ghosh et al., 2013; Zheng & Hintelmann, 2010b).

MDF; Estrade et al., 2009). The understanding of the fraction of elemental Hg in the total Hg in soils in mining areas currently remains unknown. It is speculated that elemental Hg may represent a very small fraction of total Hg in soils in this study, similar to that (<0.1%) observed in sediments in abandoned mercury mines in southwestern Alaska (Gray et al., 2000). These liquid and colloidal elemental Hg could be emitted directly under relatively higher temperature conditions (e.g., 100°C and 130°C), which in turn affect the MDF of Hg(0) isotope in temperature controlled experiments.

3.4. MIF of Hg(0) Isotope

All the experiments showed negligible MIF of the even Hg isotopes, with the even-MIF enrichment factors ($E^{200}Hg_{Hg(0)\text{-}soil} = \Delta^{200}Hg_{Hg(0)} - \Delta^{200}Hg_{soil}$) in the range of −0.03‰ to 0.09‰ (mean = 0.02 ± 0.03‰, 1 SD, $n = 50$) (Table 1). This is consistent with previous studies that anomalies of Δ^{200}Hg should be exclusively related to photochemical oxidation of Hg(0) in the atmosphere (Blum & Johnson, 2017; Chen et al., 2012; Gratz et al., 2010; Sun et al., 2016).

Significant MIF of the odd Hg isotope was observed in the emitted Hg(0) for most experiments. For the temperature-controlled experiments, Hg(0) emitted from agricultural and forest soils were all characterized by small positive Δ^{199}Hg values (0.08 to 0.34‰, $n = 22$) (Tables S1 and S2). The mean odd-MIF enrichment factor ($E^{199}Hg_{Hg(0)\text{-}soil} = \Delta^{199}Hg_{Hg(0)} - \Delta^{199}Hg_{soil}$) of agricultural soil in temperature-controlled experiments was 0.18 ± 0.04‰ (1 SD), which is comparable with that of the forest soil (0.23 ± 0.03‰, 1 SD) (Table 1), and both agree with the abiotic nonphotochemical reduction of Hg (II) in solutions and Hg liquid-vapor evaporation (0.1‰ to 0.3‰) (Estrade et al., 2009; Zheng & Hintelmann, 2009, 2010b). In addition, the slopes of the York linear regression between Δ^{199}Hg and Δ^{201}Hg of emitted Hg(0) and reactant soil for agricultural (1.55 ± 0.16, 1 SD) and forest soils (1.55 ± 0.20, 1 SD) in the temperature-controlled experiments (Figure 3) were consistent with those (1.53 to 1.63) determined or expected from abiotic nonphotochemical reduction and liquid-vapor Hg(0) evaporation (Estrade et al., 2009; Ghosh et al., 2013; Zheng & Hintelmann, 2009, 2010b), indicating the MIF of Hg isotope in temperature controls was mainly controlled by NVE.

In light- and light moisture-controlled experiments, significant positive Δ^{199}Hg (means = 0.62‰ to 0.71‰, $n = 2$) and slight positive Δ^{199}Hg (means = 0.03‰ to 0.24‰, $n = 2$) were observed in Hg(0) emitted from agricultural and forest soils, respectively (Figure 2; Tables S1 and S2). Consequently, photoreduction of Hg in agricultural and forest soils generated positive odd-MIF enrichment factors (mean $E^{199}Hg_{Hg(0)\text{-agricultural soil}}$ = 0.67‰ to 0.76‰; mean $E^{199}Hg_{Hg(0)\text{-forest soil}}$ = 0.18‰), with the exception of forest soil in the light moisture-controlled experiments (mean $E^{199}Hg_{Hg(0)\text{-forest soil}}$ = −0.03‰) (Table 1). The positive enrichment of odd Hg isotopes in the emitted Hg(0) from agricultural and forest

soils is consistent with the results of snow Hg photoreduction and S-bound Hg (II) photoreduction in solutions ($\varepsilon^{199/198}_{MIF(II-0)} = -1.0‰$) (Sherman et al., 2010; Zheng & Hintelmann, 2010a) but is opposite to the direction of MIF during the photoreduction of Hg (II) bound to sulfurless ligands (Bergquist & Blum, 2007; Zheng & Hintelmann, 2009). Abiotic nonphotochemical reduction of Hg (II) and/or Hg(0) evaporation was not likely the cause for the positive $E^{199}Hg_{Hg(0)\text{-}soil}$ because of its much lower emission flux in the absence of light at room temperature (Table S1). In addition, $\Delta^{199}Hg/\Delta^{201}Hg$ slopes were 0.99 ± 0.03 (1 SD) to 1.01 ± 0.04 (1 SD) for agricultural soil and 0.51 ± 0.36 (1 SD) to 0.89 ± 0.18 (1 SD) for forest soil in light- and light moisture-controlled experiments (Figure 3). These slopes are much lower than the slope (~1.6) for NVE fractionation but consistent with MIE fractionation (1.0 to 1.3) in photochemical reduction (Bergquist & Blum, 2007; Zheng & Hintelmann, 2009, 2010a). Therefore, the odd-MIF in light- and light moisture-controlled experiments was likely controlled by MIE fractionation in photoreduction. Zheng and Hintelmann (2010a) proposed that the net MIF of odd Hg isotopes during photoreduction is likely a combination of reduction of Hg coordinated to both sulfurless and S-containing ligands, with the former characterized by (−)MIF in Hg(0) product because photolysis is from triplet excited states, whereas the later characterized by (+)MIF in Hg(0) product because photolysis is directly from singlet excited states. Therefore, the significant positive $\Delta^{199}Hg$ indicates Hg(0) released from the agricultural soil in light- and light moisture-controlled experiments was mainly originated from species bound to S-containing ligands. This conclusion is in agreement with a speciation study that shows most of Hg in soils contaminated by drainages of mine waste in mercury mining area is in the phase of nano β-HgS (Manceau et al., 2018).

Interestingly, Hg(0) emitted from forest soil in light- and light moisture-controlled experiments showed small positive $\Delta^{199}Hg$ values (Figure 2 and Table S2). Mean $E^{199}Hg_{Hg(0)\text{-}soil}$ of forest soil were 0.18 ± 0.06 ‰ (1 SD) and −0.03 ± 0.06‰ (1 SD) in light- and light moisture-controlled experiments, respectively, which are much lower than those of agricultural soil (means = 0.67 to 0.76‰) in similar controls and slightly lower than that of forest soil in temperature control (mean = 0.23 ± 0.03‰, 1 SD) (Table 1). The small positive or negative $E^{199}Hg_{Hg(0)\text{-}soil}$ of forest soil in light- and light moisture-controlled experiments were not likely attributed to the abiotic nonphotochemical reduction of Hg (II) or Hg(0) evaporation as discussed earlier. We propose that the small positive $E^{199}Hg_{Hg(0)\text{-}soil}$ of forest soil in light-controlled experiments overall reflects a prevailing control of photoreduction of S-bound Hg (II) but the fraction of photoreduction of sulfurless ligands bound Hg (II) relative to the total Hg (II) should be higher than that in the case of the agricultural soil, yielding negative odd-MIF in Hg(0) product and reduce the magnitude of $E^{199}Hg_{Hg(0)\text{-}soil}$ of forest soil. The mechanisms associated with negative $E^{199}Hg_{Hg(0)\text{-}soil}$ of forest soil in light moisture-controlled experiments are unclear. It is speculated that the addition of water to forest soil might leach some soluble sulfurless ligands bound Hg (II) (e.g., Hg0, $HgCl_2$, and $HgSO_4$) into soil water (Bloom et al., 2003), making the magnitude of photoreduction of sulfurless ligands bound Hg (II) slightly higher than or similar to that of S-bound Hg (II), which may contribute to the small negative $E^{199}Hg_{Hg(0)\text{-}soil}$ of forest soil in light moisture control. Based on the $\Delta^{199}Hg/\delta^{202}Hg$ ratios determined from forest soil in this study and reported values observed in photoreduction of Hg (II) bound to sulfurless (1.2) and S-containing ligands (−0.77) (Bergquist & Blum, 2007; Zheng & Hintelmann, 2010a), we roughly estimate that photoreduction of Hg (II) bound to S-containing ligands contributed 61–65% for the total Hg(0) emissions from the forest soil in light- and light moisture-controlled experiments, which were lower than those estimated for the agricultural soil (79–85%).

Previous studies demonstrated that the MIF of odd Hg isotopes is affected by Hg/DOC concentration ratios (Zheng & Hintelmann, 2009, 2010a). These studies suggested that photoreduction of Hg (II) at low Hg/DOC ratios tended to increase the $\Delta^{199}Hg$ values of Hg(0) product because of the dominant bonds of Hg (II) to S-containing ligands. In this study, however, lower $E^{199}Hg_{Hg(0)\text{-}soil}$ were observed in forest soil, which had a lower Hg/NOM ratio (2.2×10^3 ng/mg) compared to the agricultural soil (5.2×10^5 ng/mg). We postulate that the inorganic- and organic-reduced sulfur groups are abundant in agricultural rice paddy soils (Li et al., 2019; Rothenberg & Feng, 2012), which could be derived from cinnabar ores and waste and lead to a major complexation of Hg (II) with S-containing ligands (Manceau et al., 2018). In the forest soil, sulfurless (O/N) groups are much more abundant than reduced sulfur groups (O'Donnell et al., 2016). Therefore, there is likely more bonding of Hg (II) with sulfurless ligands in the forest soil than the agricultural soil, which generates (−)MIF of Hg(0) product and subsequently results in lower or slightly negative $E^{199}Hg_{Hg(0)\text{-}soil}$ in the forest soil in light and light moisture controlled experiments.

4. Conclusions and Implications

In this study, fractionation of Hg isotopes during emission of Hg(0) from Hg-enriched agricultural and forest soils in Wanshan Hg mining area was investigated under a variety of laboratory-controlled conditions. Soil emitted Hg(0) was all characterized by significant negative δ^{202}Hg values (means = −4.48‰ to −1.68‰, n = 6) in light-, light moisture-, and temperature-controlled experiments and generated negative shift in δ^{202}Hg (means = −3.38‰ to −1.34‰, n = 6) in emitted Hg(0) relative to reactant soils. A large variation in odd-MIF during emission of Hg(0) was observed. $E^{199}Hg_{Hg(0)\text{-}soil}$ of agricultural and forest soils showed slightly positive values (means = 0.18‰ to 0.23‰, n = 2) in temperature controls, which were likely controlled by abiotic nonphotochemical reduction and/or Hg(0) evaporation processes. Emission of Hg(0) from agricultural soil in light and light moisture controls generated larger positive $E^{199}Hg_{Hg(0)\text{-}soil}$ (means = 0.67 and 0.76, respectively), suggesting Hg(0) was mainly derived from the photoreduction of Hg (II) bound to S-containing ligands. However, the $E^{199}Hg_{Hg(0)\text{-}soil}$ during Hg(0) emissions from forest soil were much smaller in light control (mean = 0.18 ± 0.06‰, 1 SD) and slightly negative in light moisture control (mean = −0.03 ± 0.06‰, 1 SD), which may have been attributed to the increasing photoreduction of sulfurless ligands bound Hg (II).

Hg isotope fractionation during Hg(0) emission from soil plays an important role in the isotopic signatures of Hg in global reservoirs (Sonke, 2011). Since Hg mining and retorting activities have been completely prohibited in many Hg mining areas, soil emissions could then represent an important source of atmospheric Hg(0) in Hg mining areas. Given the measured isotopic compositions of Hg(0) emitted from agricultural and forest soils in this study, negative δ^{202}Hg and positive Δ^{199}Hg signatures of atmospheric Hg(0) could be expected in Hg mining areas, which agrees well the hypothesis based on leaf Hg isotope composition in the New Idria Hg mine (Wiederhold et al., 2013). Our data also indicate that Hg(0) emissions from soils in Hg mining areas would potentially lead a negative shift of δ^{202}Hg and a positive shift of Δ^{199}Hg in regional and atmospheric Hg(0) pool, given that soil Hg(0) emissions in naturally enriched and mining areas are an important source of atmospheric Hg (Agnan et al., 2016). However, we admittedly acknowledge that, due to the reverse odd-MIF induced by different types of NOM, the isotopic composition of emitted Hg(0) should be site specific. Our results therefore cannot fully represent the isotopic signatures of Hg(0) emitted from the global soils. In addition, it should be noted that our observations are primarily representative of Hg isotope fractionation associated with Hg(0) emission, whereas soil-atmosphere Hg exchange is a bidirectional process. The isotope fractionation of Hg during the its soil-atmosphere exchange could also be affected by many other processes including adsorption and oxidation of Hg(0) as well as other abiotic and biotic transformations. Therefore, the "realistic" fractionation of Hg isotope during the soil-atmosphere Hg exchange is a combination of specific isotope fractionations related to different environmental processes, which might be different from the present study. Hence, there is a need to better constrain the specific and net Hg isotope fractionation during the exchange of Hg between atmosphere and different types of soil. This would help to understand the role of soil-atmosphere exchange in the distribution of Hg stable isotope in atmospheric and continental reservoirs. In addition, such progresses could also be used to identify the processes and factors controlling the soil-atmosphere Hg exchange.

Conflict of Interest

The authors state that there is no conflict of interests.

Data Availability Statement

Data sets for this research can be found in a public domain repository (http://www.dx.doi.org/10.11922/sciencedb.00144).

Acknowledgments

This work was supported by the Strategic Priority Research Program (Grant No. XDB40000000) and Key Research Program of Frontier Sciences, CAS (Grant No: ZDBS-LY-DQC029), the National Nature Science Foundation of China (U1612442, 41622305, and 41473025), the Youth Innovation Promotion Association CAS (2017443), and the K.C. Wong Education Foundation.

References

Agnan, Y., Le Dantec, T., Moore, C. W., Edwards, G. C., & Obrist, D. (2016). New constraints on terrestrial surface atmosphere fluxes of gaseous elemental mercury using a global database. *Environmental Science & Technology*, *50*(2), 507–524. https://doi.org/10.1021/acs.est5b04013

AMAP/UNEP (2013). Geospatially distributed mercury emissions dataset 2010v1, edited.

Bergquist, B. A., & Blum, J. D. (2007). Mass-dependent and -independent fractionation of Hg isotopes by photoreduction in aquatic systems. *Science*, *318*(5849), 417–420. https://doi.org/10.1126/science.1148050

Biswas, A., Blum, J. D., Lammers, A., & Douglas, T. (2008). Isotopic evidence for changing sources of mercury to the Arctic. *Geochimica et Cosmochimica Acta*, *72*(12), A86–A86.

Bloom, N. S., Preus, E., Katon, J., & Hiltner, M. (2003). Selective extractions to assess the biogeochemically relevant fractionation of inorganic mercury in sediments and soils. *Analytica Chimica Acta*, *479*(2), 233–248. https://doi.org/10.1016/S0003-2670(02)01550-7

Blum, J. D., & Bergquist, B. A. (2007). Reporting of variations in the natural isotopic composition of mercury. *Analytical and Bioanalytical Chemistry*, *388*(2), 353–359. https://doi.org/10.1007/s00216-007-1236-9

Blum, J. D., & Johnson, M. W. (2017). Recent developments in mercury stable isotope analysis. *Reviews in Mineralogy and Geochemistry*, *82*(1), 733–757. https://doi.org/10.2138/rmg.2017.82.17

Blum, J. D., Sherman, L. S., & Johnson, M. W. (2014). Mercury isotopes in earth and environmental sciences. *Annual Review of Earth and Planetary Sciences*, *42*(1), 249–269. https://doi.org/10.1146/annurev-earth-050212-124107

Buchachenko, A. L., Kouznetsov, D. A., & Shishkov, A. V. (2004). Spin biochemistry: Magnetic isotope effect in the reaction of creatine kinase with CH3HgCl. *The Journal of Physical Chemistry. A*, *108*(5), 707–710. https://doi.org/10.1021/jp030450o

Chen, J. B., Hintelmann, H., Feng, X. B., & Dimock, B. (2012). Unusual fractionation of both odd and even mercury isotopes in precipitation from Peterborough, ON, Canada. *Geochimica et Cosmochimica Acta*, *90*, 33–46. https://doi.org/10.1016/j.gca.2012.05.005

Choi, H. D., & Holsen, T. M. (2009). Gaseous mercury fluxes from the forest floor of the Adirondacks. *Environmental Pollution*, *157*(2), 592–600. https://doi.org/10.1016/j.envpol.2008.08.020

Demers, J. D., Blum, J. D., & Zak, D. R. (2013). Mercury isotopes in a forested ecosystem: Implications for air-surface exchange dynamics and the global mercury cycle. *Global Biogeochemical Cycles*, *27*(1), 222–238. https://doi.org/10.1002/Gbc.20021

Dreyfr, R. M. (1939). Darkening of cinnabar in sunlight. *American Mineralogist*, *24*(7), 457–460.

Enrico, M., Le Roux, G., Marusczak, N., Heimburger, L. E., Claustres, A., Fu, X. W., et al. (2016). Atmospheric mercury transfer to peat bogs dominated by gaseous elemental mercury dry deposition. *Environmental Science & Technology*, *50*(5), 2405–2412. https://doi.org/10.1021/acs.est.5b06058

Estrade, N., Carignan, J., & Donard, O. F. X. (2010). Isotope tracing of atmospheric mercury sources in an urban area of northeastern France. *Environmental Science & Technology*, *44*(16), 6062–6067. https://doi.org/10.1021/Es100674a

Estrade, N., Carignan, J., Sonke, J. E., & Donard, O. F. X. (2009). Mercury isotope fractionation during liquid-vapor evaporation experiments. *Geochimica et Cosmochimica Acta*, *73*(10), 2693–2711. https://doi.org/10.1016/j.gca.2009.01.024

Fantozzi, L., Ferrara, R., Dini, F., Tamburello, L., Pirrone, N., & Sprovieri, F. (2013). Study on the reduction of atmospheric mercury emissions from mine waste enriched soils through native grass cover in the Mt. Amiata region of Italy. *Environmental Research*, *125*, 69–74. https://doi.org/10.1016/j.envres.2013.02.004

Feng, X. B., Yin, R. S., Yu, B., & Du, B. Y. (2013). Mercury isotope variations in surface soils in different contaminated areas in Guizhou Province, China. *Chinese Science Bulletin*, *58*(2), 249–255. https://doi.org/10.1007/s11434-012-5488-1

Fu, X., Zhang, H., Liu, C., Zhang, H., Lin, C.-J., & Feng, X. (2019). Significant seasonal variations in isotopic composition of atmospheric total gaseous mercury at forest sites in China caused by vegetation and mercury sources. *Environmental Science & Technology*, *53*(23), 13,748–13,756. https://doi.org/10.1021/acs.est.9b05016

Fu, X. W., Heimburger, L. E., & Sonke, J. E. (2014). Collection of atmospheric gaseous mercury for stable isotope analysis using iodine- and chlorine-impregnated activated carbon traps. *Journal of Analytical Atomic Spectrometry*, *29*(5), 841–852. https://doi.org/10.1039/C3ja50356a

Fu, X. W., Zhang, H., Feng, X. B., Tan, Q. Y., Ming, L. L., Liu, C., & Zhang, L. M. (2019). Domestic and transboundary sources of atmospheric particulate bound mercury in remote areas of China: Evidence from mercury isotopes. *Environmental Science & Technology*, *53*(4), 1947–1957. https://doi.org/10.1021/acs.est.8b06736

Ghosh, S., Schauble, E. A., Couloume, G. L., Blum, J. D., & Bergquist, B. A. (2013). Estimation of nuclear volume dependent fractionation of mercury isotopes in equilibrium liquid-vapor evaporation experiments. *Chemical Geology*, *336*, 5–12. https://doi.org/10.1016/j.chemgeo.2012.01.008

Gratz, L. E., Keeler, G. J., Blum, J. D., & Sherman, L. S. (2010). Isotopic composition and fractionation of mercury in Great Lakes precipitation and ambient air. *Environmental Science & Technology*, *44*(20), 7764–7770. https://doi.org/10.1021/Es100383w

Gray, J. E., Theodorakos, P. M., Bailey, E. A., & Turner, R. R. (2000). Distribution, speciation, and transport of mercury in stream-sediment, stream-water, and fish collected near abandoned mercury mines in southwestern Alaska, USA. *Science of the Total Environment*, *260*(1–3), 21–33. https://doi.org/10.1016/S0048-9697(00)00539-8

Gustin, M. S., Ericksen, J. A., Schorran, D. E., Johnson, D. W., Lindberg, S. E., & Coleman, J. S. (2004). Application of controlled mesocosms for understanding mercury air-soil-plant exchange. *Environmental Science & Technology*, *38*(22), 6044–6050. https://doi.org/10.1021/Es0487933

Gustin, M. S., Lindberg, S., Marsik, F., Casimir, A., Ebinghaus, R., Edwards, G., et al. (1999). Nevada STORMS project: Measurement of mercury emissions from naturally enriched surfaces. *Journal of Geophysical Research*, *104*(D17), 21,831–21,844. https://doi.org/10.1029/1999jd900351

Gustin, M. S., & Stamenkovic, J. (2005). Effect of watering and soil moisture on mercury emissions from soils. *Biogeochemistry*, *76*(2), 215–232. https://doi.org/10.1007/s10533-005-4566-8

Gustin, M. S., Taylor, G. E., & Maxey, R. A. (1997). Effect of temperature and air movement on the flux of elemental mercury from substrate to the atmosphere. *Journal of Geophysical Research*, *102*(D3), 3891–3898. https://doi.org/10.1029/96JD02742

Holmes, C. D., Jacob, D. J., Corbitt, E. S., Mao, J., Yang, X., Talbot, R., & Slemr, F. (2010). Global atmospheric model for mercury including oxidation by bromine atoms. *Atmospheric Chemistry and Physics*, *10*(24), 12,037–12,057. https://doi.org/10.5194/acp-10-12037-2010

Jew, A. D., Kim, C. S., Rytuba, J. J., Gustin, M. S., & Brown, G. E. (2011). New technique for quantification of elemental Hg in mine wastes and its implications for mercury evasion into the atmosphere. *Environmental Science & Technology*, *45*(2), 412–417. https://doi.org/10.1021/es1023527

Jiskra, M., Marusczak, N., Leung, K. H., Hawkins, L., Prestbo, E., & Sonke, J. E. (2019). Automated stable isotope sampling of gaseous elemental mercury (ISO-GEM): Insights into GEM emissions from building surfaces. *Environmental Science & Technology*, *53*(8), 4346–4354. https://doi.org/10.1021/acs.est.8b06381

Jiskra, M., Sonke, J. E., Agnan, Y., Helmig, D., & Obrist, D. (2019). Insights from mercury stable isotopes on terrestrial-atmosphere exchange of Hg(0) in the Arctic tundra. *Biogeosciences*, *16*(20), 4051–4064. https://doi.org/10.5194/bg-16-4051-2019

Jiskra, M., Wiederhold, J. G., Bourdon, B., & Kretzschmar, R. (2012). Solution speciation controls mercury isotope fractionation of Hg (II) sorption to goethite. *Environmental Science & Technology*, *46*(12), 6654–6662. https://doi.org/10.1021/es3008112

Jiskra, M., Wiederhold, J. G., Skyllberg, U., Kronberg, R. M., Hajdas, I., & Kretzschmar, R. (2015). Mercury deposition and re-emission pathways in boreal Forest soils investigated with Hg isotope signatures. *Environmental Science & Technology*, *49*(12), 7188–7196. https://doi.org/10.1021/acs.est.5b00742

Kritee, K., Blum, J. D., & Barkay, T. (2008). Mercury stable isotope fractionation during reduction of Hg (II) by different microbial pathways. *Environmental Science & Technology*, *42*(24), 9171–9177. https://doi.org/10.1021/Es801591k

Li, Y. Y., Wang, Y. J., Zhang, Q. J., Hu, W. J., Zhao, J. T., Chen, Y. H., et al. (2019). Elemental sulfur amendment enhance methylmercury accumulation in rice (*Oryza sativa* L.) grown in Hg mining polluted soil. *Journal of Hazardous Materials*, *379*. https://doi.org/10.1016/j.jhazmat.2019.05.094

Lin, H. Y., Yuan, D. X., Lu, B. Y., Huang, S. Y., Sun, L. M., Zhang, F., & Gao, Y. Q. (2015). Isotopic composition analysis of dissolved mercury in seawater with purge and trap preconcentration and a modified Hg introduction device for MC-ICP-MS. *Journal of Analytical Atomic Spectrometry*, *30*(2), 353–359. https://doi.org/10.1039/C4JA00242C

Lindberg, S., Bullock, R., Ebinghaus, R., Engstrom, D., Feng, X. B., Fitzgerald, W., et al. (2007). A synthesis of progress and uncertainties in attributing the sources of mercury in deposition. *Ambio*, *36*(1), 19–33. https://doi.org/10.1579/0044-7447(2007)36[19:ASOPAU]2.0.CO;2

Lindberg, S. E., Zhang, H., Gustin, M., Vette, A., Marsik, F., Owens, J., et al. (1999). Increases in mercury emissions from desert soils in response to rainfall and irrigation. *Journal of Geophysical Research*, *104*(D17), 21,879–21,888. https://doi.org/10.1029/1999JD900202

Manceau, A., Wang, J. X., Rovezzi, M., Glatzel, P., & Feng, X. B. (2018). Biogenesis of mercury-sulfur nanoparticles in plant leaves from atmospheric gaseous mercury. *Environmental Science & Technology*, *52*(7), 3935–3948. https://doi.org/10.1021/acs.est.7b05452

Meng, B., Feng, X. B., Qiu, G. L., Li, Z. G., Yao, H., Shang, L. H., & Yan, H. Y. (2016). The impacts of organic matter on the distribution and methylation of mercury in a hydroelectric reservoir in Wujiang River, Southwest China. *Environmental Toxicology and Chemistry*, *35*(1), 191–199. https://doi.org/10.1002/etc.3181

Moore, C., & Carpi, A. (2005). Mechanisms of the emission of mercury from soil: Role of UV radiation. *Journal of Geophysical Research*, *110*, D24302. https://doi.org/10.1029/2004JD005567

Motta, L. C., Kritee, K., Blum, J. D., Tsz-Ki Tsui, M., & Reinfelder, J. R. (2020). Mercury isotope fractionation during the photochemical reduction of Hg (II) coordinated with organic ligands. *The Journal of Physical Chemistry A*, *124*(14), 2842–2853. https://doi.org/10.1021/acs.jpca.9b06308

O'Donnell, J. A., Aiken, G. R., Butler, K. D., Guillemette, F., Podgorski, D. C., & Spencer, R. G. M. (2016). DOM composition and transformation in boreal forest soils: The effects of temperature and organic-horizon decomposition state. *Journal of Geophysical Research: Biogeosciences*, *121*, 2727–2744. https://doi.org/10.1002/2016JG003431

Qiu, G. L., Feng, X. B., Wang, S. F., & Shang, L. H. (2005). Mercury and methylmercury in riparian soil, sediments, mine-waste calcines, and moss from abandoned Hg mines in east Guizhou province, southwestern China. *Applied Geochemistry*, *20*(3), 627–638. https://doi.org/10.1016/j.apgeochem.2004.09.006

Rothenberg, S. E., & Feng, X. B. (2012). Mercury cycling in a flooded rice paddy. *Journal of Geophysical Research*, *117*, G03003. https://doi.org/10.1029/2011JG001800

Salminen, R., Demetriades, A., & Reeder, S. (2005). Geochemical Atlas of Europe, Part I: Background Information, Methodology and Maps, Geological Survey of Finland.

Schauble, E. A. (2007). Role of nuclear volume in driving equilibrium stable isotope fractionation of mercury, thallium, and other very heavy elements. *Geochimica et Cosmochimica Acta*, *71*(9), 2170–2189. https://doi.org/10.1016/j.gca.2007.02.004

Schluter, K. (2000). Review: evaporation of mercury from soils. An integration and synthesis of current knowledge. *Environmental Geology*, *39*(3–4), 249–271. https://doi.org/10.1007/s002540050005

Selin, N. E. (2009). Global biogeochemical cycling of mercury: A review. *Annual Review of Environment and Resources*, *34*(1), 43–63. https://doi.org/10.1146/annurev.environ.051308.084314

Sherman, L. S., Blum, J. D., Johnson, K. P., Keeler, G. J., Barres, J. A., & Douglas, T. A. (2010). Mass-independent fractionation of mercury isotopes in Arctic snow driven by sunlight. *Nature Geoscience*, *3*(3), 173–177. https://doi.org/10.1038/Ngeo758

Smith, R. S., Wiederhold, J. G., Jew, A. D., Brown, G. E., Bourdon, B., & Kretzschmar, R. (2015). Stable Hg isotope signatures in creek sediments impacted by a former Hg mine. *Environmental Science & Technology*, *49*(2), 767–776. https://doi.org/10.1021/es503442p

Sonke, J. E. (2011). A global model of mass independent mercury stable isotope fractionation. *Geochimica et Cosmochimica Acta*, *75*(16), 4577–4590. https://doi.org/10.1016/j.gca.2011.05.027

Sonke, J. E., & Blum, J. D. (2013). Advances in mercury stable isotope biogeochemistry Preface. *Chemical Geology*, *336*, 1–4. https://doi.org/10.1016/j.chemgeo.2012.10.035

Streets, D. G., Horowitz, H. M., Lu, Z., Levin, L., Thackray, C. P., & Sunderland, E. M. (2019). Global and regional trends in mercury emissions and concentrations, 2010–2015. *Atmospheric Environment*, *201*, 417–427. https://doi.org/10.1016/j.atmosenv.2018.12.031

Sun, G., Sommar, J., Feng, X., Lin, C.-J., Ge, M., Wang, W., et al. (2016). Mass-dependent and -independent fractionation of mercury isotope during gas-phase oxidation of elemental mercury vapor by atomic Cl and Br. *Environmental Science & Technology*, *50*(17), 9232–9241. https://doi.org/10.1021/acs.est.6b01668

Sun, R. Y., Enrico, M., Heimburger, L. E., Scott, C., & Sonke, J. E. (2013). A double-stage tube furnace-acid-trapping protocol for the preconcentration of mercury from solid samples for isotopic analysis. *Analytical and Bioanalytical Chemistry*, *405*(21), 6771–6781. https://doi.org/10.1007/s00216-013-7152-2

Sun, R. Y., Jiskra, M., Amos, H. M., Zhang, Y. X., Sunderland, E. M., & Sonke, J. E. (2019). Modelling the mercury stable isotope distribution of Earth surface reservoirs: Implications for global Hg cycling. *Geochimica et Cosmochimica Acta*, *246*, 156–173. https://doi.org/10.1016/j.gca.2018.11.036

USEPA (2002). Method 1631, revision E: Mercury in water by oxidation, purge and trap, and cold vapor atomic fluorescence spectrometry, United States Environmental Protection Agency, 10–46.

Wang, S. F., Feng, X. B., Qiu, G. G., Shang, L. H., Li, P., & Wei, Z. Q. (2007). Mercury concentrations and air/soil fluxes in Wuchuan mercury mining district, Guizhou province, China. *Atmospheric Environment*, *41*(28), 5984–5993. https://doi.org/10.1016/j.atmosenv.2007.03.013

Wang, S. F., Feng, X. B., Qiu, G. L., Fu, X. W., & Wei, Z. Q. (2007). Characteristics of mercury exchange flux between soil and air in the heavily air-polluted area, eastern Guizhou, China. *Atmospheric Environment*, *41*(27), 5584–5594. https://doi.org/10.1016/j.atmosenv.2007.03.002

Wang, X., Luo, J., Yin, R. S., Yuan, W., Lin, C. J., Sommar, J., et al. (2017). Using mercury isotopes to understand mercury accumulation in the Montane Forest floor of the eastern Tibetan Plateau. *Environmental Science & Technology*, *51*(2), 801–809. https://doi.org/10.1021/acs.est.6b03806

Wiederhold, J. G., Cramer, C. J., Daniel, K., Infante, I., Bourdon, B., & Kretzschmar, R. (2010). Equilibrium mercury isotope fractionation between dissolved Hg (II) species and thiol-bound Hg. *Environmental Science & Technology*, *44*(11), 4191–4197. https://doi.org/10.1021/es100205t

Wiederhold, J. G., Smith, R. S., Siebner, H., Jew, A. D., Brown, G. E., Bourdon, B., & Kretzschmar, R. (2013). Mercury isotope signatures as tracers for Hg cycling at the New Idria Hg mine. *Environmental Science & Technology*, *47*(12), 6137–6145. https://doi.org/10.1021/Es305245z

Yang, L., & Sturgeon, R. (2009). Isotopic fractionation of mercury induced by reduction and ethylation. *Analytical and Bioanalytical Chemistry*, *393*(1), 377–385. https://doi.org/10.1007/s00216-008-2348-6

Yin, R. S., Feng, X. B., Foucher, D., Shi, W. F., Zhao, Z. Q., & Wang, J. (2010). High precision determination of mercury isotope ratios using online mercury vapor generation system coupled with multi-collector inductively coupled plasma-mass spectrometry. *Chinese Journal of Analytical Chemistry*, *38*(7), 929–934. https://doi.org/10.3724/Sp.J.1096.2010.00929

Yin, R. S., Feng, X. B., Wang, J. X., Li, P., Liu, J. L., Zhang, Y., et al. (2013). Mercury speciation and mercury isotope fractionation during ore roasting process and their implication to source identification of downstream sediment in the Wanshan mercury mining area, SW China. *Chemical Geology*, *336*, 72–79. https://doi.org/10.1016/j.chemgeo.2012.04.030

York, D., Evensen, N. M., Martinez, M. L., & Delgado, J. D. (2004). Unified equations for the slope, intercept, and standard errors of the best straight line. *American Journal of Physics*, *72*(3), 367–375. https://doi.org/10.1119/1.1632486

Yuan, W., Sommar, J., Lin, C.-J., Wang, X., Li, K., Liu, Y., et al. (2019). Stable isotope evidence shows re-emission of elemental mercury vapor occurring after reductive loss from foliage. *Environmental Science & Technology*, *53*(2), 651–660. https://doi.org/10.1021/acs.est.8b04865

Zhang, H., & Lindberg, S. E. (1999). Processes influencing the emission of mercury from soils: A conceptual model. *Journal of Geophysical Research*, *104*(D17), 21,889–21,896. https://doi.org/10.1029/1999JD900194

Zheng, W., Demers, J. D., Lu, X., Bergquist, B. A., Anbar, A. D., Blum, J. D., & Gu, B. (2018). Mercury stable isotope fractionation during abiotic dark oxidation in the presence of thiols and natural organic matter. *Environmental Science & Technology*, *53*(4), 1853–1862. https://doi.org/10.1021/acs.est.8b05047

Zheng, W., Foucher, D., & Hintelmann, H. (2007). Mercury isotope fractionation during volatilization of Hg(0) from solution into the gas phase. *Journal of Analytical Atomic Spectrometry*, *22*(9), 1097–1104. https://doi.org/10.1039/B705677j

Zheng, W., & Hintelmann, H. (2009). Mercury isotope fractionation during photoreduction in natural water is controlled by its Hg/DOC ratio. *Geochimica et Cosmochimica Acta*, *73*(22), 6704–6715. https://doi.org/10.1016/j.gca.2009.08.016

Zheng, W., & Hintelmann, H. (2010a). Isotope fractionation of mercury during its photochemical reduction by low-molecular-weight organic compounds. *The Journal of Physical Chemistry. A*, *114*(12), 4246–4253. https://doi.org/10.1021/jp9111348

Zheng, W., & Hintelmann, H. (2010b). Nuclear field shift effect in isotope fractionation of mercury during abiotic reduction in the absence of light. *The Journal of Physical Chemistry. A*, *114*(12), 4238–4245. https://doi.org/10.1021/jp910353y

Zheng, W., Obrist, D., Weis, D., & Bergquist, B. A. (2016). Mercury isotope compositions across north American forests. *Global Biogeochemical Cycles*, *30*(10), 1475–1492. https://doi.org/10.1002/2015GB005323

Zhu, W., Lin, C. J., Wang, X., Sommar, J., Fu, X. W., & Feng, X. B. (2016). Global observations and modeling of atmosphere-surface exchange of elemental mercury: A critical review. *Atmospheric Chemistry and Physics*, *16*(7), 4451–4480. https://doi.org/10.5194/acp-16-4451-2016